

Features of thermal radiation of one-dimensional photonic structures on an absorbing substrate

V.P. Maslov, V.O. Morozhenko, N.V. Kachur

V. Lashkaryov Institute of Semiconductor Physics, NAS of Ukraine
41, prospect Nauky, 03680 Kyiv, Ukraine; e-mail: morozh@meta.ua

Abstract. The dependences of the thermal radiation (TR) lines contrast and amplitude of the systems (photonic structure)/substrate on the optical characteristics of both the photonic structure and the substrate have been investigated theoretically and experimentally. As it has been ascertained, these dependences demonstrate non-monotonic behavior, and the characteristics of the system TR can both increase and decrease depending on the ratio of individual optical parameters of the system components. The results of theoretical research were confirmed by experimental studies of TR systems Ge/GaAs, Ge/GaAs/Al, GaAs/Au and GaAs/(opaque substrate). The results of the research can be used in the development of narrow-band emitters for the middle and far IR range, which can be applied in the optical infrared devices for a wide range of applications.

Keywords: photonic bandgap materials, one-dimensional photonic structures, thermal radiation, infrared sources.

<https://doi.org/10.15407/spqeo24.04.444>

PACS 42.70.Qs, 42.72.Ai, 44.40.+a, 78.30.-j

Manuscript received 17.06.21; revised version received 18.07.21; accepted for publication 10.11.21; published online 23.11.21.

1. Introduction

Recent years, close attention has been paid to the study of thermal radiation (TR) of one-dimensional single-layer and multilayer photonic structures (PS). Their optical properties are related not so much to the properties of the constituent materials but to the interferential effects within the structure. Due to interaction of electromagnetic waves with the periodic structure, TR of these structures has the features of coherence: it has a selective spectrum and a petal pattern. The relevance of PS TR research is due to the search for new materials for creation of radiation exchange enhancing coatings [1–5], narrow-band sources for the middle and far IR ranges [3, 5–8], stealth coatings [3, 10–12] *etc.*

In [1], it was proposed a multilayer of $\text{SiO}_2/\text{Si}_3\text{N}_4$ selective IR emitter with the spectral characteristic optimized for radiative cooling through radiative emission of heat to ambient space. Photonic structures used to enhance radiative energy exchange in the organisms were researched in [2]. A selective emitter designed on the dielectric layer as one unit cell has been proposed in [3]. It can be used as a passive radiative cooler, or as a selective IR emitter within the spectral band 5.5...7.6 μm . In [4, 5], the reviews of photonic structures application for radiative cooling and some other energy application opportunities of them have been presented.

In [6], it is shown that the thermal excitation of plasmon-polariton on a surface of a titanium nitride 1D grating produces a well-collimated mid-infrared radiation. The article [7] provides the theoretical and experimental research of the spectral and directional radiative properties of the Fabry–Perot optical cavities and periodic Ag and Au gratings on silicon. A wide range of applications for these structures has been proposed. The study [8] of SiO_2 based Fabry–Perot structures at various temperatures showed that TR spectra of such emitters exhibit peak broadening and shifting with temperature increases. The review article [5] also presents the possibilities of using the photonic structures as the narrow-band IR emitters as well.

The structures described in [3] exhibit high reflectivity in the spectral bands of 3...5 and 8...14 μm and can significantly improve the capability of infrared stealth. In [9], it was studied the possibility of using the multilayer photonic films $(\text{Ge}/\text{ZnS})_3/\text{Ge}/(\text{Ge}/\text{ZnS})_3/\text{ZnS}$ to achieve invisibility in the 5...8 μm band. One-dimensional Ge/ TiO_2 photonic structures, with low infrared-emissivity in the 8...14 μm band, were successfully designed and prepared in [10]. An optically transparent ITO/dielectric/ITO sandwiched structure with simultaneous high-efficiency microwave absorptivity and low IR emissivity is proposed in [11]. Good results of compatible stealth in both radio and infrared ranges are shown

in [12] by using the structure $(\text{Ge}/\text{ZnSe})^2/(\text{Si}/\text{ZnSe})/(\text{Ge}/\text{ZnSe})^3$. The results showed a high average reflectance in IR waveband 8...14 μm and strong absorption in radar band frequency between 7.8 and 18 GHz.

This work aimed at theoretical and experimental investigations of the characteristics inherent to TR of the single-layer and multilayer photonic structures placed on an incoherent absorbing substrate. It includes studying the influence of absorption, reflectance and TR of the substrate on the TR characteristics of the whole system structure/substrate (PS/S).

2. Model and basic relations

Let us consider the system consisting of a one-dimensional photonic structure and an incoherent substrate, as it is shown schematically in Fig. 1. PS contains one layer with non-zero absorption located between two non-absorptive mirrors with reflectance R_1 and R_2 . In a general case, the mirrors R_1 , R_2 can be both non-absorbing Bragg structures with air-layer and layer-substrate interfaces, respectively. Let the layer be characterized by a thickness d_l , refractive index η_l and absorption coefficient α_l . The substrate is characterized by a refractive index η_s and absorption coefficient α_s .

According to the Kirchhoff law, the intensity of thermal radiation emitted by a heated system along the normal to their surface is

$$P = P_{bb}(1 - R - T), \quad (1)$$

where T and R are, respectively, the transmittance and reflectance of the system, P_{bb} is a radiation intensity of the black body under the same conditions. In the case of normal incidence of external light on the system from the side of the structure, as it is shown in Fig. 1, T and R are described by the following analytical expressions [13]:

$$T = \frac{T_p \eta_s (1 - R_3)}{1 - \eta_s^2 R_p R_3}, \quad R = R_p + \frac{T_p^2 \eta_s^2 R_3}{1 - \eta_s^2 R_p R_3}. \quad (2)$$

Here,

$$T_p = \frac{(1 - R_1)(1 - R_2)\eta_l}{1 - 2G \cos 2\delta + G^2}, \quad (3)$$

$$R_p = \frac{R_1 - 2G \cos 2\delta + R_2 \eta_l^2}{1 - 2G \cos 2\delta + G^2} \quad (4)$$

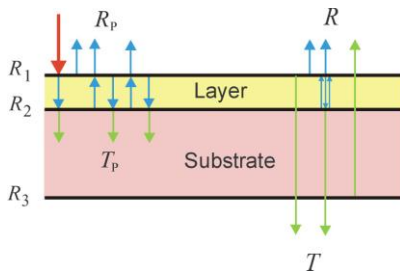


Fig. 1. Schematic representation of light distribution in a system (photonic structure)/substrate.

are the transmittance and reflectance of the photonic structure, $\eta_l = \exp(-\alpha_l d_l)$ and $\eta_s = \exp(-\alpha_s d_s)$ are, respectively, the internal transmittance of the layer and substrate, $\delta = 2\pi n_l d_l / \lambda$, $G = \eta_l \sqrt{R_1 R_2}$. If the mirrors R_1 , R_2 and R_3 are the Bragg ones, their reflectances are calculated using the known transfer matrix method [14].

3. Results and discussion

3.1. Theoretical results

Fig. 2 shows a dependence of an interference contrast ($V = (P_M - P_m)/(P_M + P_m)$, where P_M , P_m are the adjacent interferential maximum and minimum, respectively) of the system structure/substrate TR on the transmission and reflection coefficient of the substrate back side. For comparative analysis, the TR contrast of the system is normalized to the contrast of a free PS (V_p). As can be seen, a change in the parameters of the substrate leads to both an increase and a decrease in the contrast. The value of V reaches its maximum when $\eta_s = 1$ and $R_3 = 0.5$, when the substrate does not emit and half of TR emitted by PS in the opposite direction is re-reflected to the emitting surface.

The TR contrast reaches its minimum value when $\eta_s \approx 0.75$ and $R_3 = 1$. With these parameters, a sufficient amount of PS radiation reflects from the mirror R_3 and returns to the emitting surface. However, TR of PS is added to TR of the incoherent substrate. This reduces the contrast of the interference oscillations of total TR.

Fig. 3 shows a 3D plot of the dependence of the TR oscillation amplitude ($\Delta P = P_M - P_m$) of the PS/S system on the internal transmittances of the substrate and PS. ΔP is normalized to the TR intensity of the black body. It is seen, when the structure is opaque ($\eta_l = 0$), $\Delta P = 0$ within the entire range of η_s variation. TR of the system does not contain interferential extrema and is similar to TR of ordinary gray body.

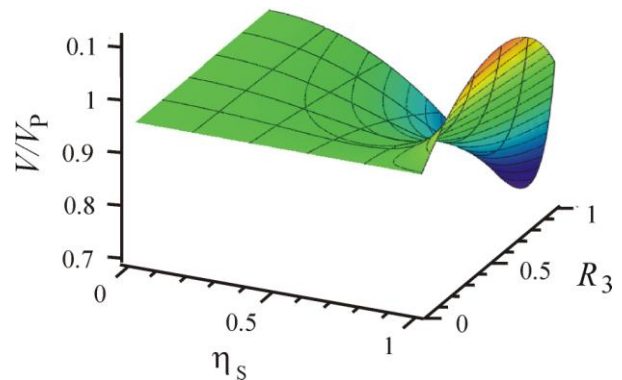


Fig. 2. Dependence of the TR interference pattern contrast of the PS/S system on the internal transmittance and the back side reflectance of the substrate. The system TR contrast is normalized to the TR contrast of free PS. The following PS parameters were used in the calculations: $\eta_l = 0.9$; $R_1 = R_2 = 0.3$.

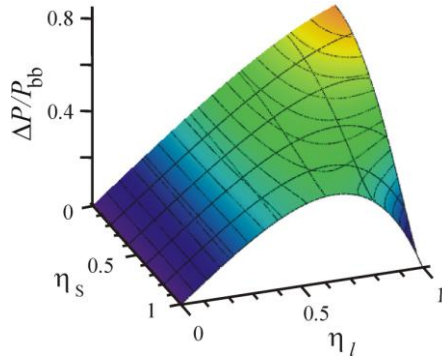


Fig. 3. Dependence of the TR oscillation amplitude of the system PS/S on the internal transmittances of the substrate and PS. The following system parameters were used in the calculations: $R_1 = R_2 = 0.3$, $R_3 = 1$.

When $\eta_l \neq 0$, the dependence $\Delta P(\eta_l)$ has a different character depending on the fixed values of η_s . In the case of a transparent substrate ($\eta_s = 1$), the dependence $\Delta P(\eta_l)$ has a nonmonotonic character with a maximum and zero values at the beginning and end ($\Delta P(0) = \Delta P(1) = 0$). This is due to the fact that in the case of a non-absorbing system, there are no radiative energy transitions in it. As the absorption of the substrate increases, the oscillation amplitude of the system TR increases. Under these conditions, the system TR exists and exhibits interferential properties at $\eta_l = 1$ due to interaction of the substrate TR with the photonic structure. When the transmittance of the substrate exceeds a certain value (with the parameters of the system used in the calculations this is $\eta_s \approx 0.6$), $\Delta P(\eta_l)$ loses its non-monotonic form and approaches linear form. The value ΔP reaches its maximum when the layer is transparent ($\eta_l = 1$) and the substrate is opaque ($\eta_s \approx 0$).

3.2. Experimental results

Fig. 4 shows the experimental TR spectra of a coherent p -Ge layer on an n -GaAs substrate. The layer thickness was $d_l = 12.4 \mu\text{m}$. As known, the absorption of p -Ge almost does not change with the wavelength within the spectral range $8 \dots 30 \mu\text{m}$ [15], while the absorption coefficient of n -GaAs depends on the wavelength in proportional to λ^3 [16]. This enables to study the dependence of the parameters of the system on the internal transmittance of the substrate with the remaining optical parameters of the system unchanged. The curve 1 shows the TR spectrum of the structure with a clean back side of the substrate (Ge/GaAs system). The curve 2 shows the TR spectrum of the same sample but with an aluminum layer deposited on the back side of the substrate (Ge/GaAs/Al system, $R_3 \approx 1$).

As seen, the system with a nontransmitting mirror has the maximum TR intensity. However, when the wavelength increases, the spectrum approaches the TR spectrum of a system with a clean back surface.

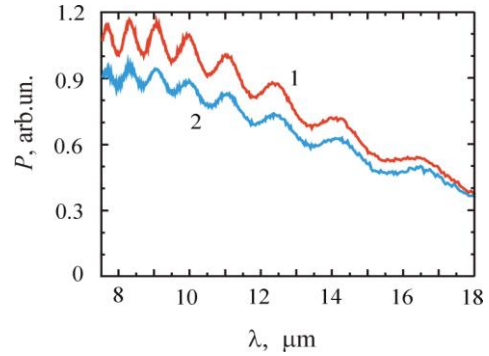


Fig. 4. Thermal radiation spectra: 1 – Ge layer on a GaAs substrate; 2 – Ge layer on a GaAs substrate with an aluminum layer on the reverse side. $d_l = 12.4 \mu\text{m}$. The system temperature was equal to 370 K.

This is due to the increased absorption of the substrate. At $\lambda \approx 18 \mu\text{m}$, the substrate becomes opaque and these spectra merge.

Fig. 5 shows the dependences of the TR interferential patterns contrasts of the Ge/GaAs system (curve 1) and the Ge/GaAs/Al system (curve 2) on the GaAs substrate internal transmittance. The values of η_s have been obtained from the transmission and reflection spectra of the system by using the elements of the methods [13, 17, 18]. The corresponding wavelengths are shown on the upper scale.

Since the neighboring TR extrema are strongly separated in wavelengths, to determine the contrasts, a polynomial approximation of the maximum and minimum points was used. The values of the contrasts were calculated using the equations:

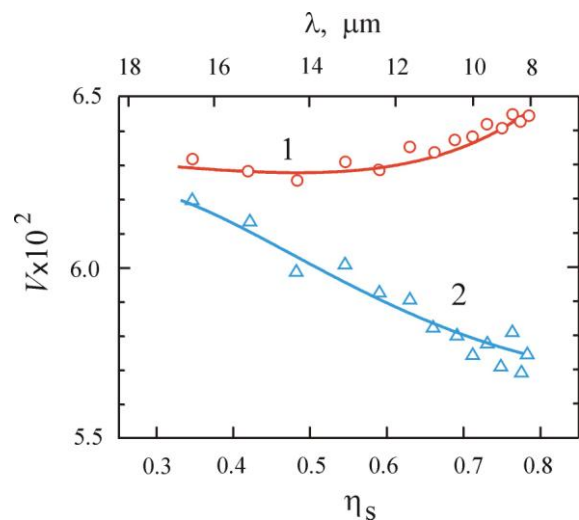


Fig. 5. Dependences of the TR interference patterns contrasts of on the internal transmittance of the substrate (the upper scale shows the corresponding wavelength). 1 – Ge layer on a GaAs substrate; 2 – Ge layer on a GaAs substrate with an aluminum layer on the reverse side. $d_l = 12.4 \mu\text{m}$.

$$V|_{\lambda_M} = \frac{P_M(\lambda_M) - \rho_m(\lambda_M)}{P_M(\lambda_M) + \rho_m(\lambda_M)},$$

$$V|_{\lambda_m} = \frac{\rho_M(\lambda_m) - P_m(\lambda_m)}{\rho_M(\lambda_m) + P_m(\lambda_m)}, \quad (5)$$

where λ_M and λ_m are wavelengths corresponding to the interferences maxima and minima of TR, respectively, $\rho_M(\lambda)$, $\rho_m(\lambda)$ are, respectively, the upper and lower envelopes functions obtained by polynomial approximation of the points P_M and P_m .

It can be seen, at a high value of the substrate internal transmittance, the TR contrast of the Ge/GaAs system exceeds the contrast of the Ge/GaAs/Al system. When the value of η_S decreases, it decreases, too. The contrast of the Ge/GaAs/Al system, on the contrary, increases with decreasing η_S (increasing the wavelength). Such behavior of TR contrasts of these structures is qualitatively consistent with the theoretical one (see Fig. 2).

Fig. 6 shows the experimental dependences of the TR interference lines amplitude of a coherent *n*-GaAs plate with the different substrates on the internal transmittance of the plate. The values of η_l were determined from the analysis of the transmission and reflection spectra of the used plate [17, 18]. The corresponding wavelengths are shown on the upper scale of the figure. ΔP was determined using a linear interpolation with nodes at the points of the corresponding extrema [13].

As seen, the dependence $\Delta P(\eta_l)$ of a plate with a gold coating on the reverse side (GaAs/Au system, points and curve 1) has a nonmonotonic form with a maximum at $\eta_l \approx 0.62$. This is due to the following: when the layer is opaque ($\eta_l = 0$), there is no interference in the system and the amplitude of the interference lines is zero.

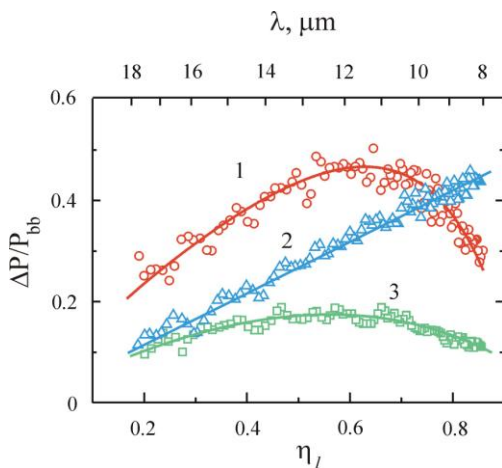


Fig. 6. Dependences of the TR oscillations amplitude of a coherent *n*-GaAs plate ($N \approx 4 \cdot 10^{17} \text{ cm}^{-1}$, $d_l = 10^{-2} \text{ cm}$) on the internal transmittance of the plate. 1 – system GaAs/Au; 2 – system GaAs/(opaque substrate); 3 – free plate GaAs. The oscillation amplitude is normalized to the TR intensity of the blackbody. The upper scale shows the corresponding TR wavelength.

When the layer is transparent ($\eta_l = 1$) and $R_2 \approx 1$, there is no thermal radiation. This also leads to the disappearance of the TR lines. Thus, in a system with a strongly reflecting rear mirror, there are optimal conditions for emission, at which the amplitude of the TR lines is maximal.

The points and curve 2 show the dependence $\Delta P(\eta_l)$ of a free GaAs plate placed on an opaque substrate. As can be seen, in this case, the dependence $\Delta P(\eta_l)$ is monotonic and close to linear. The oscillation amplitude of the TR lines of the system GaAs/(opaque substrate) is less than that of the system GaAs/Au due to the lower Q-factor of the resonator. However, at high values of the plate transmission, it begins to exceed ΔP of the system GaAs/Au. This is explained by the presence of the substrate TR, which contribution to the total radiation of the system increases with increasing η_l . This explanation is confirmed by the dependence $\Delta P(\eta_l)$ of a free plate without a substrate (points and curve 3). As can be seen, in the absence of an emitting substrate, the amplitude of the TR lines is less, and the dependence $\Delta P(\eta_l)$ is similar to that of the system GaAs/Au. In this case, the optimal conditions for emission occur at $\eta_l \approx 0.5$.

The obtained experimental dependences $\Delta P(\eta_l)$ of systems with reflective, absorbing and transparent (absent) substrates are in good agreement with the results of theoretical calculations presented in Fig. 3.

4. Conclusions

In the paper, the influence of the final substrate on the thermal radiation characteristics of the whole system (photon structure)/substrate has been investigated theoretically and experimentally. It has been ascertained that the contrast and amplitude of the system TR in a non-trivial way depend on the ratio of the optical characteristics of the photon structure and the substrate.

Systems consisting of a *p*-Ge layer on a GaAs substrate and a coherent GaAs plate on a reflective and absorbing substrates were used in experimental studies. In the first case, the dependence of the TR contrast on the substrate internal transmittances with constant absorption of the layer has been investigated. In the second case, the dependence of the TR lines amplitude on the internal transmittances of the coherent layer at constant optical parameters of the substrate has been studied. It is ascertained that when the transparency of substrate increases, the contrast of the interferences pattern of the TR system increases in the case of a not high reflection coefficient of the rear side of the system ($R_3 \approx 0.3$) and decreases at $R_3 \approx 1$. The dependence of the TR interferences lines amplitude on the photon structure internal transmittances has a non-monotonic form with a maximum in the case of a weakly emitting substrate and is close to an increasing linear one, when the substrate has intensive TR. The obtained experimental results are in good agreement with the presented results of theoretical research.

The results of the work can be used for development of narrow-band emitters in the middle and far IR range for the needs of IR spectroscopy, environmental monitoring systems, optical devices for gas analysis and analysis of the composition of the substance *etc.* The obtained results can also be useful in designing of the radiation exchange enhancing coatings and stealth coatings with minimal emissivity in the thermal range of wavelengths.

References

1. Ma H., Yao K., Dou S. *et al.* Multilayered SiO₂/Si₃N₄ photonic emitter to achieve high-performance all-day radiative cooling. *Sol. Energy Mater. Sol. Cells.* 2020. **212**. P. 110584-1–110584-7. <https://doi.org/10.1016/j.solmat.2020.110584>.
2. Vasiljević D., Pavlović D., Lazović V. *et al.* Thermal radiation management by natural photonic structures: *Morimus asper funereus* case. *J. Therm. Biol.* 2021. **98**. P. 102932-1–102932-10. <https://doi.org/10.1016/j.jtherbio.2021.102932>.
3. Xu C., Qu S., Pang Y. *et al.* Metamaterial absorber for frequency selective thermal radiation. *Infrared Phys. Technol.* 2018. **88**. P. 133–138. <https://doi.org/10.1016/j.infrared.2017.08.017>.
4. Li W., Fan S. Nanophotonic control of thermal radiation for energy applications. *Opt. Exp.* 2018. **26**. P. 15995–16021. <https://doi.org/10.1364/OE.26.015995>.
5. Fan S. Thermal photonics and energy applications. *Joule.* 2017. **1**, No 2. P. 264–273. <https://doi.org/10.1016/j.joule.2017.07.012>.
6. Liu J.J., Guler U., Lagutchev A. *et al.* Quasi-coherent thermal emitter based on refractory plasmonic materials. *Opt. Mater. Exp.* 2015. **5**, No 12. P. 2721–2728. <https://doi.org/10.1364/OME.5.002721>.
7. Zhang Z.M., Wang L.P. Measurements and modeling of the spectral and directional radiative properties of micro/nanostructured materials. *Int. J. Thermophys.* 2013. **34**. P. 2209–2242. <https://doi.org/10.1007/s10765-011-1036-5>.
8. Wang L.P., Basu S. and Zhang Z.M. Direct measurement of thermal emission from a Fabry-Perot cavity resonator. *J. Heat Transfer.* 2012. **134**. P. 072701-1–072701-9. <https://doi.org/10.1115/1.4006088>.
9. Zhang W., Lv D. Preparation and characterization of Ge/TiO₂ one-dimensional photonic crystal with low infrared-emissivity in the 8–14 μm band. *Mater. Res. Bull.* 2020. **124**. P. 110747-1–110747-4. <https://doi.org/10.1016/j.materresbull.2019.110747>.
10. Xu C., Wang B., Yan M. *et al.* An optically transparent sandwich structure for radar-infrared bistealth. *Infrared Phys. Technol.* 2020. **105**. P. 103108-1–103108-11. <https://doi.org/10.1016/j.infrared.2019.103108>.
11. Chen X., Tian Ch., Chen T. Composite grating structure for laser and infrared compatible stealth with high visible transmittance. *Optik.* 2019. **183**. P. 863-868. <https://doi.org/10.1016/j.ijleo.2019.03.007>
12. Liu B., Shi J.-M., Zhang J.K. *et al.* Infrared stealth performance analysis of photonic crystal with high heat dissipation. *Opt. Mater.* 2021. **111**. P. 110689-1–110689-5. <https://doi.org/10.1016/j.optmat.2020.110689>.
13. Zhang J.-K., Shi J.-M., Zhao D.-P. *et al.* Realization of compatible stealth material for infrared, laser and radar based on one-dimensional doping-structure photonic crystals. *Infrared Phys. Technol.* 2017. **85**. P. 62–65. <https://doi.org/10.1016/j.infrared.2017.05.018>.
14. Morozhenko V.O., Maslov V.P., Bariakhtar I.V., Kachur N.V. Determination of the parameters of coherent magneto-optical layers on a finite absorbing substrate from thermal radiation spectra. *SPQEO.* 2020. **23**. P. 400–407. <https://doi.org/10.15407/spqeo23.04.400>.
15. Furman Sh.A., Tikhonravov A.V. *Basics of Optics of Multilayer Systems.* Edition Frontiers, Gif-sur-Yvette, 1992.
16. Kaiser W., Collins R.J., and Fan H.Y. Infrared absorption in *p*-type germanium. *Phys. Rev.* 1953. **91**. P. 1380–1381. <https://doi.org/10.1103/PhysRev.91.1380>.
17. Spitzer W.G. and Whelan J.M. Infrared absorption and electron effective mass in *n*-type gallium arsenide. *Phys. Rev.* 1959. **114**. P. 59–63. <https://doi.org/10.1103/PhysRev.114.59>.
18. Shaabana E.R., Yahiab I.S., El-Metwally E.G. Validity of Swanepoel's method for calculating the optical constants of thick films. *Acta Phys. Pol. A.* 2012. **121**. P. 628–635. <https://doi.org/10.12693/APhysPolA.121.628>.
19. Lévêque G. and Villachon-Renard Y. Determination of optical constants of thin film from reflectance spectra. *Appl. Opt.* 1990. **29**. P. 3207–3212. <https://doi.org/10.1364/AO.29.003207>.

Authors and CV



Volodymyr Maslov, Doctor of Materials Science, Head of the Department of physics and technological basics of sensor materials at the V. Lashkaryov Institute of Semiconductor Physics. Professor at the National Technical University of Ukraine “Igor Sikorsky Kyiv Polytechnic Institute” since 2010. Honored inventor of Ukraine. Author of more than 156 publications and more than 400 patents of Ukraine and USSR author's certificates. His research interests include several topics of optical engineering and physical behavior of functional materials as well as phenomena of surface plasmon resonance with application of it in medicine and ecology. <https://orcid.org/0000-0001-7795-6156>
E-mail: vpmaslov@ukr.net



Vasyl Morozhenko, PhD in Physics and Mathematics, Senior Researcher at the Department of physics and technological basics of sensor materials science, V. Lashkaryov Institute of Semiconductor Physics. Author of more than 50 publications. The area of his scientific interests includes infrared spectroscopy, optical properties of semiconductors, photonics and magnetophotonics.

<https://orcid.org/0000-0003-4228-995X>

E-mail: morozh@meta.ua



Nataliya Kachur got her degree MS in Physics and Techniques at the National Aviation University of Ukraine, Mechanical faculty in 2006. The area of her scientific interests includes physics of surfaces, development and design sensors for applying in control of quality of transparent materials.

<https://orcid.org/0000-0001-6868-8452>

E-mail: natalyakachur@gmail.com

Особливості теплового випромінювання одновимірних фотонних структур на поглинаючій підкладці

В.П. Маслов, В.О. Мороженко, Н.В. Качур

Анотація. У роботі теоретично та експериментально досліджено залежності контрасту та амплітуди ліній теплового випромінювання (ТВ) системи (фотонна структура)/підкладка від оптичних характеристик фотонної структури та підкладки. З'ясовано, що ці залежності мають немонотонний вигляд, і характеристики ТВ системи можуть як збільшуватись, так і зменшуватись у залежності від співвідношення окремих оптичних параметрів складових системи. Результати теоретичних досліджень були підтверджені експериментальними дослідженнями ТВ систем Ge/GaAs, Ge/GaAs/Al, GaAs/Au та GaAs/(непрозора підкладка). Результати досліджень можуть знайти застосування при розробці вузькосмугових випромінювачів середнього та дальнього ІЧ-діапазону для оптичних інфрачервоних приладів широкого спектра застосувань.

Ключові слова: одновимірні фотонні структури, теплове випромінювання, інфрачервоні випромінювачі.